British Journal of Pharmacology

DOI:10.1111/bph.12596
www.brjpharmacol.org

RESEARCH PAPER

Modulation of $K_{2P}2.1$ and $K_{2P}10.1$ K^+ channel sensitivity to carvedilol by alternative mRNA translation initiation

J Kisselbach[1], C Seyler[1], P A Schweizer[1], R Gerstberger[2], R Becker[1], H A Katus[1] and D Thomas[1]

[1]*Department of Cardiology, Medical University Hospital, Heidelberg, Germany, and* [2]*Institute for Veterinary Physiology and Biochemistry, Justus-Liebig-University, Giessen, Germany*

Correspondence
Dierk Thomas, Department of Cardiology, University of Heidelberg, Im Neuenheimer Feld 410, D-69120 Heidelberg, Germany. E-mail: dierk.thomas@med.uni-heidelberg.de

Received
28 August 2013
Revised
20 December 2013
Accepted
16 January 2014

BACKGROUND AND PURPOSE

The β-receptor antagonist carvedilol blocks a range of ion channels. $K_{2P}2.1$ (TREK1) and $K_{2P}10.1$ (TREK2) channels are expressed in the heart and regulated by alternative translation initiation (ATI) of their mRNA, producing functionally distinct channel variants. The first objective was to investigate acute effects of carvedilol on human $K_{2P}2.1$ and $K_{2P}10.1$ channels. Second, we sought to study ATI-dependent modulation of K_{2P} K^+ current sensitivity to carvedilol.

EXPERIMENTAL APPROACH

Using standard electrophysiological techniques, we recorded currents from wild-type and mutant $K_{2P}2.1$ and $K_{2P}10.1$ channels in *Xenopus* oocytes and HEK 293 cells.

KEY RESULTS

Carvedilol concentration-dependently inhibited $K_{2P}2.1$ channels ($IC_{50,oocytes}$ = 20.3 μM; $IC_{50,HEK}$ = 1.6 μM) and this inhibition was frequency-independent. When $K_{2P}2.1$ isoforms generated by ATI were studied separately in oocytes, the IC_{50} value for carvedilol inhibition of full-length channels (16.5 μM) was almost 5-fold less than that for the truncated channel variant (IC_{50} = 79.0 μM). Similarly, the related $K_{2P}10.1$ channels were blocked by carvedilol ($IC_{50,oocytes}$ = 24.0 μM; $IC_{50,HEK}$ = 7.6 μM) and subject to ATI-dependent modulation of drug sensitivity.

CONCLUSIONS AND IMPLICATIONS

Carvedilol targets $K_{2P}2.1$ and $K_{2P}10.1$ K^+ channels. This previously unrecognized mechanism supports a general role of cardiac K_{2P} channels as antiarrhythmic drug targets. Furthermore, the work reveals that the sensitivity of the cardiac ion channels $K_{2P}2.1$ and $K_{2P}10.1$ to block was modulated by alternative mRNA translation initiation.

Abbreviations

ATI, alternative translation initiation; K_{2P}, two-pore-domain K^+ channel; TREK, TWIK-related K^+ channel; TWIK, tandem of P domains in a weak inward rectifying K^+ channel

Introduction

Two-pore-domain potassium (K_{2P}) channels stabilize the resting membrane potential and facilitate action potential repolarization (channel nomenclature follows Alexander *et al.*, 2013). Dynamic and polymodal regulation of K_{2P} currents determines cellular excitability (Goldstein *et al.*, 2001; Gierten *et al.*, 2008; 2012; Thomas *et al.*, 2008; Sandoz *et al.*,

2011; Staudacher *et al.*, 2011a; Kisselbach *et al.*, 2012; Rahm *et al.*, 2012; 2014; Seyler *et al.*, 2012). In the heart, $K_{2P}3.1$ inhibition or genetic inactivation of $K_{2P}3.1$ currents results in action potential prolongation, suggesting that these channels might represent targets for antiarrhythmic therapy (Putzke *et al.*, 2007; Gierten *et al.*, 2010; Ravens, 2010; Decher *et al.*, 2011; Donner *et al.*, 2011; Limberg *et al.*, 2011; Staudacher *et al.*, 2011b; Petric *et al.*, 2012; Schmidt *et al.*, 2012). Prolongation of action potentials and cardiac effective refractory periods is a characteristic of class III antiarrhythmic drugs, reducing membrane excitability and decreasing arrhythmia susceptibility. In addition to $K_{2P}3.1$, expression of $K_{2P}2.1$ (TREK1, TWIK-related K^+ channel) channels has been shown in atria and ventricles at mRNA, protein and functional levels (Fink *et al.*, 1996; Reyes *et al.*, 1998; Aimond *et al.*, 2000; Medhurst *et al.*, 2001; Terrenoire *et al.*, 2001; Liu and Saint, 2004; Tan *et al.*, 2004; Li *et al.*, 2006; Zhang *et al.*, 2008; Decher *et al.*, 2011; Zhao *et al.*, 2011; Goonetilleke and Quayle, 2012; Schmidt *et al.*, 2014). The closely related $K_{2P}10.1$ (TREK2) channels have been detected in the heart as well (Medhurst *et al.*, 2001; Liu and Saint, 2004; Li *et al.*, 2006; Staudacher *et al.*, 2011a; Gierten *et al.*, 2012). However, data delineating the cardiac functions of $K_{2P}2.1$ and $K_{2P}10.1$ channels are limited. Synthesis of different K_{2P} proteins with different N terminal domains from a single mRNA by alternative mRNA translation initiation (ATI) was recently revealed as a novel mechanism to increase the number of functional TREK protein subunits, producing two ($K_{2P}2.1$) or three ($K_{2P}10.1$) endogenous variants (Simkin *et al.*, 2008; Thomas *et al.*, 2008). ATI regulates K_{2P} current magnitude, ion selectivity and intersubunit interactions (Simkin *et al.*, 2008; Thomas *et al.*, 2008; Veale *et al.*, 2010; Eckert *et al.*, 2011). Effects of ATI on K_{2P} channel sensitivity to antiarrhythmic drugs have not been investigated to date.

Carvedilol is a non-selective β-adrenoreceptor antagonist with a multichannel blocking pharmacological profile. Carvedilol targets a variety of ion currents including K^+ channels (Karle *et al.*, 2001; Staudacher *et al.*, 2011b). The clinical use of carvedilol is associated with reduced morbidity and mortality in heart failure patients (Poole-Wilson *et al.*, 2003; Remme *et al.*, 2007). In addition, suppression of atrial fibrillation and ventricular tachyarrhythmia as well as pronounced prolongation of atrial and ventricular effective refractory periods suggest specific antiarrhythmic effects of the drug (Senior *et al.*, 1992; Brunvand *et al.*, 1996; Cice *et al.*, 2000; Takusagawa *et al.*, 2000; Katritsis *et al.*, 2003; Merritt *et al.*, 2003; Ramaswamy, 2003; Acikel *et al.*, 2008; Kanoupakis *et al.*, 2008).

We hypothesized that inhibition of $K_{2P}2.1$ and $K_{2P}10.1$ background currents contributed to the antiarrhythmic effect of carvedilol. Furthermore, this study was designed to investigate modulation of the drug sensitivity of cardiac K_{2P} channels by ATI.

Methods

Molecular biology

Human cDNAs encoding wild-type and mutant $K_{2P}2.1$ (TREK1b) (GenBank accession number, EF165335) were kindly provided by Dr. Steve Goldstein (Brandeis University, Waltham, MA, USA) (Thomas *et al.*, 2008). Human $K_{2P}2.1$ was amplified from a heart cDNA library (Clontech, Palo Alto, CA, USA), inserted into the pCR2.1-TOPO vector (Invitrogen, Carlsbad, CA, USA) and subcloned into pMAX, a dual-purpose expression vector containing a CMV promoter for mammalian expression and a T7 promoter for cRNA synthesis. Human $K_{2P}10.1$ (TREK2c) (GenBank accession number EU978939) was amplified from a brain cDNA library as described (Gierten *et al.*, 2008; Staudacher *et al.*, 2011a). Complementary DNA was inserted into the pCR2.1-TOPO vector and subcloned into pRAT, a dual-purpose expression vector containing a CMV promoter for mammalian expression and a T7 promoter for cRNA synthesis (Bockenhauer *et al.*, 2001). Generation of mutant $K_{2P}2.1$ and $K_{2P}10.1$ clones was previously reported (Thomas *et al.*, 2008; Staudacher *et al.*, 2011a). Briefly, $K_{2P}2.1$ and $K_{2P}10.1$ mutations described in the text were made with the QuikChange Site-Directed Mutagenesis kit (Stratagene, La Jolla, CA, USA). N terminal channel truncation was achieved using PCR. All cDNA constructs were confirmed by DNA sequencing. Complementary RNAs were transcribed after vector linearization using T7 RNA polymerase and the mMessage mMachine kit (Ambion, Austin, TX, USA). Transcripts were quantified by spectrophotometry and cRNA integrity was assessed by agarose gel electrophoresis.

Oocyte preparation and injection

All animal care and experimental procedures complied with the Directive 2010/63/EU of the European Parliament and the United States National Institutes of Health Guide for the Care and Use of Laboratory Animals (NIH Publication no. 85-23, revised 1996). Approval was granted by the local Animal Welfare Committee (reference number A-38/11). All studies involving animals are reported in accordance with the ARRIVE guidelines for reporting experiments involving animals (Kilkenny *et al.*, 2010; McGrath *et al.*, 2010). The preparation of oocytes has been reported earlier in detail (Gierten *et al.*, 2008; Staudacher *et al.*, 2011b; Seyler *et al.*, 2012). Briefly, oocytes were isolated from *Xenopus laevis* ovarian lobes after surgical removal under tricaine anaesthesia (1 $g \cdot L^{-1}$; pH 7.5). Oocyte collection was alternated between left and right ovaries, and a maximum of three surgeries were performed on one individual frog. After the final collection of oocytes, anaesthetized frogs were killed by decerebration and pithing. Complementary RNA (0.1–25 ng; 46 nl per oocyte) was injected into stage V–VI defolliculated *Xenopus* oocytes.

Cell culture

HEK 293 cells were cultured in DMEM (Invitrogen) supplemented with 10% FBS, 2 mM L-glutamine, 100 000 $U \cdot L^{-1}$ penicillin and 100 $mg \cdot L^{-1}$ streptomycin in an atmosphere of 95% humidified air and 5% CO_2 at 37°C. Cells were passaged regularly. Transient transfections (5 µg cDNA/35 mm dish) were performed using FuGENE HD transfection reagent (Promega, Madison, WI, USA) according to the manufacturer's instructions.

Electrophysiology

Whole-cell currents were recorded from *Xenopus* oocytes using two-electrode voltage-clamp electrophysiology with an

Oocyte Clamp amplifier (Warner Instruments, Hamden, CT, USA) and pCLAMP9 (Axon Instruments, Foster City, CA, USA) software 2–3 days after injection, as described (Thomas *et al.*, 2008; Gierten *et al.*, 2012). Data were sampled at 2 kHz and filtered at 1 kHz. Electrodes were filled with 3 M KCl. The extracellular solution contained 96 mM NaCl, 4 mM KCl, 1.1 mM $CaCl_2$, 1 mM $MgCl_2$, 5 mM HEPES (pH 7.4, adjusted with NaOH).

Whole-cell patch-clamp recordings from HEK 293 cells were carried out using a RK-400 amplifier (Bio-Logic SAS, Claix, France) as reported (Gierten *et al.*, 2008; Schmidt *et al.*, 2012; Seyler *et al.*, 2012). Electrodes were filled with the following solution: 100 mM K-aspartate, 20 mM KCl, 2 mM $MgCl_2$, 1 mM $CaCl_2$, 10 mM EGTA, 10 mM HEPES, 40 mM glucose, 5 mM K-ATP (pH adjusted to 7.2 with KOH). The external solution for these experiments was composed of 140 mM NaCl, 5 mM KCl, 1 mM $MgCl_2$, 1.8 mM $CaCl_2$, 10 mM HEPES, 10 mM glucose (pH adjusted to 7.4 with NaOH). Identification of transfected cells was performed by requiring outward current amplitudes of at least 200 pA and leak currents of ≤10% of the initial maximum current. Recordings were carried out under constant perfusion at room temperature, and no leak subtraction was done during the experiments.

Drug administration

Carvedilol, metoprolol and propranolol (all from Sigma-Aldrich, St. Louis, MO, USA) were prepared as 100 mM stock solutions in DMSO (carvedilol, propranolol) or H_2O (metoprolol) and stored at –20°C. On the day of experiments, aliquots of the stock solutions were diluted to the desired concentrations with the bath solution. Wild-type and mutant $K_{2P}2.1$ or $K_{2P}10.1$ currents recorded from *Xenopus* oocytes were not significantly altered upon application of 0.1% DMSO (v^*v^{-1}; maximum bath concentration) for 20 min (n = 4 to 10 cells were studied for each channel, $P > 0.05$).

Biochemistry

Pooled tissue-specific (heart, brain, aorta, lung, skeletal muscle, stomach, small intestine, kidney, uterus and prostate) total protein samples ('Protein Medleys') were obtained commercially from Clontech (Mountain View, CA, USA). The samples (30 µg per well) were subjected to SDS-PAGE on precast 10% gels ('Ready Gels', Bio-Rad, Hercules, CA, USA), followed by wet-transfer onto nitrocellulose paper and immunoblot analysis using anti-$K_{2P}2.1$ antibodies raised against recombinant C terminal rat $K_{2P}2.1$ protein containing 68 amino acids (1:400; Thomas *et al.*, 2008). Successful detection of human $K_{2P}2.1$ protein using this antibody has been demonstrated previously (Thomas *et al.*, 2008). Secondary fluorescence-labelled goat anti-rabbit antibodies were used at 1:5000 dilutions, and secondary labelling of fluorescent conjugates was documented with an Odyssey scanner (Li-Cor Biosciences, Lincoln, NE, USA).

Data analysis

Origin (OriginLab, Northampton, MA, USA) software was used for data analysis. Data are expressed as mean ± SEM. Concentration-response relationships for drug-induced block were fit with a Hill equation of the following form: $I_{drug}/I_{control} = 1/[1 + (D/IC_{50})^n]$, where I indicates current, D is the drug concentration, n is the Hill coefficient and IC_{50} is the concentration necessary for 50% block. We applied paired and unpaired Student's t-tests (two-tailed tests) to compare statistical significance of the results: $P < 0.05$ was considered statistically significant. The multiple comparisons shown in Figure 2F and in Table 3 were performed using one-way ANOVA. If the hypothesis of equal means could be rejected at the 0.05-level, pair-wise comparisons of groups were made and the probability values were adjusted for multiple comparisons using the Bonferroni correction.

Results

Inhibition of human cardiac $K_{2P}2.1$ (TREK1) channels by carvedilol

Carvedilol blockade of $hK_{2P}2.1$ channels was investigated in *Xenopus laevis* oocytes. From a holding potential of –80 mV, pulses were applied for 500 ms to voltages between –140 and +60 mV in 20 mV increments (0.5 Hz). Representative families of current traces from one cell are shown for control conditions (Figure 1A) and after application of 100 µM carvedilol for 20 min (Figure 1B). Current amplitudes were analysed at the end of the 0 mV test pulse. After a control period (20 min) with no significant amplitude changes ($I_{0\,min}$, 3.17 ± 0.4 µA; $I_{20\,min}$, 3.08 ± 0.4 µA; n = 14; P = 0.18), currents decreased concentration-dependently after administration of carvedilol (Figure 1A–D) and the derived IC_{50} value is shown in Table 1, with a Hill coefficient, n_H, of 1.6 ± 0.1 (n = 12 to 15 cells were studied at each concentration). Blockade of $K_{2P}2.1$ channels in oocytes was incomplete with maximum current reduction of 80.3 ± 2.2% by 300 µM (20 min) carvedilol (Figure 1C), similar to dronedarone inhibition of $K_{2P}2.1$ reported earlier (Schmidt *et al.*, 2012). The onset of block was rapid (Figure 1D) and 100 µM carvedilol inhibited $K_{2P}2.1$ currents by 76.3 ± 1.9% (n = 6; P = 0.001). Inhibitory effects were partially reversible, as current levels reached 50.0 ± 2.7% of controls, 20 min after removal of the drug. We cannot exclude a minor contribution of the bath solution exchange (usually requiring ~0.5–1 min) to the kinetics of block and unblock shown in Figure 1D. Mean voltages required to achieve 50% of maximum K_{2P} current amplitudes recorded at +60 mV ($V_{50\%,K2P}$) yielded 23.1 ± 0.5 mV under control conditions and 22.8 ± 0.4 mV after application of 100 µM carvedilol (n = 15; P = 0.36; Figure 1E,F). We observed an apparent increase of relative (but not absolute) inward currents compared with outward currents in the presence of carvedilol (Figure 1E,F). As low levels of endogenous currents (at hyperpolarizing pulses) are not blocked by carvedilol, they are expected to become more apparent in relation to significantly blocked $K_{2P}2.1$ currents at more depolarized potentials. Similar findings were obtained with $K_{2P}10.1$ channels.

$K_{2P}2.1$ currents show outward (or open) rectification. Linear ramp voltage protocols were applied between –140 and +60 mV (500 ms) before and after application of 100 µM carvedilol (20 min) to assess drug effects on current rectification (Figure 2A). The currents displayed outward rectification before and after carvedilol administration. The degree of blockade at +20 mV ramp potential was 80.5 ± 1.3% (n = 4;

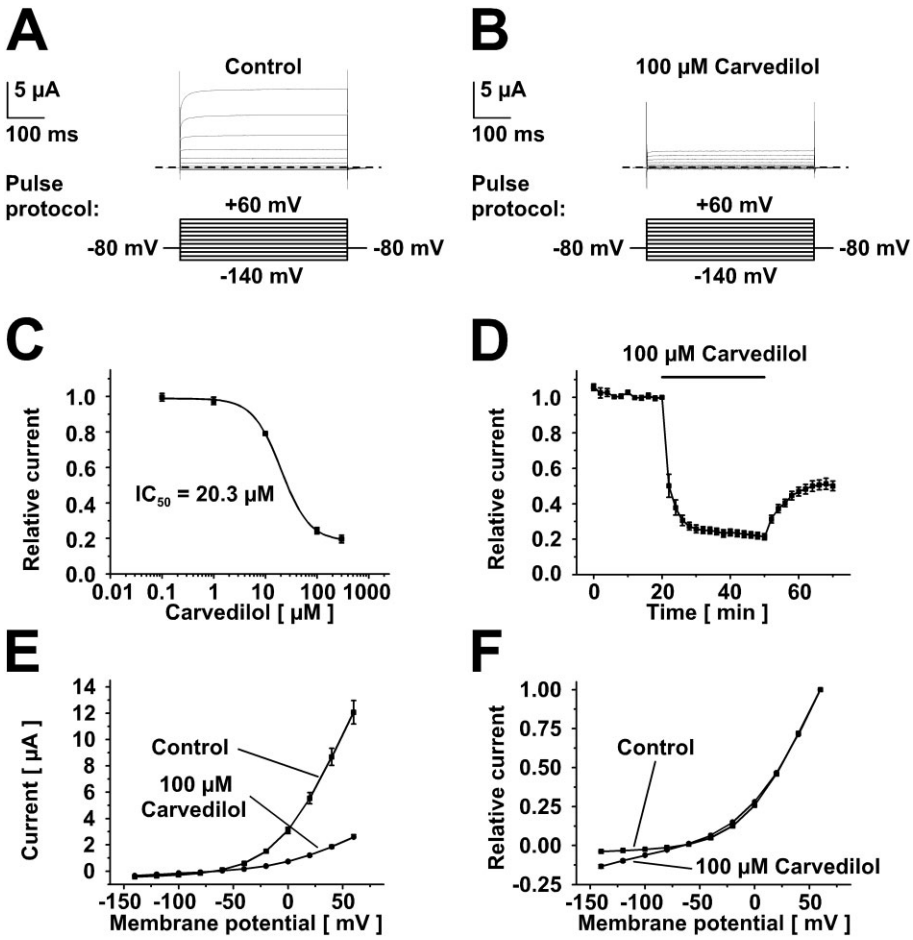

Figure 1

Inhibition of human $K_{2P}2.1$ (TREK1) channels by carvedilol in *Xenopus laevis* oocytes. (A, B) Representative macroscopic currents recorded under control conditions and after application of 100 µM carvedilol. Zero current levels are indicated by dashed lines. (C) Concentration-response relationships for the effect of carvedilol on $K_{2P}2.1$ currents measured at the end of the 0 mV voltage step (n = 12 to 15 cells). (D) Time course of $hK_{2P}2.1$ current blockade by 100 µM carvedilol (n = 6). Panels E and F display *I–V* relationships (i.e. mean current amplitudes as function of the test pulse potential) recorded under isochronal conditions (E, original current amplitudes; F, values normalized to maximum currents; n = 15).

P = 0.001). Next, carvedilol block was investigated using extended voltage pulse durations. $K_{2P}2.1$ currents were recorded during a single depolarizing step to +20 mV for 7.5 s under control conditions and after application of 100 µM carvedilol for 20 min while keeping the membrane potential at −80 mV (Figure 2B). Current inhibition during the first 400 ms of the protocol is displayed with linear and logarithmic time scales in Figure 2C and D. Analysis of channel block after carvedilol administration revealed that significant inhibition of $hK_{2P}2.1$ channels had occurred at −80 mV, indicated by the level of block at the beginning of the depolarizing pulse (60.2 ± 2.3%; n = 8; P < 0.0001) (Figure 2C,D). A second, time-dependent component of block was observed during the +20 mV-pulse (block at 400 ms: 72.2 ± 1.0%; n = 8; P < 0.0001), similar to ~76% inhibition observed above with 500 ms-voltage steps.

To study frequency-dependence of block, human $K_{2P}2.1$ channels were rapidly activated by a depolarizing step to +20 mV (500 ms) at intervals of 2 or 10 s, respectively. Current reduction by 30 µM carvedilol was plotted versus time (Figure 2E). The degree of inhibition after 20 min was not significantly different (P = 0.079) between 0.5 Hz (53.0 ± 0.9%; n = 7; P = 0.002) and 0.1 Hz stimulation rate (58.2 ± 2.6%; n = 7; P = 0.001). Finally, the specificity of $K_{2P}2.1$ current block was investigated. Compared with carvedilol, $K_{2P}2.1$ displayed reduced affinity to the selective β-adrenoceptor antagonist metoprolol (100 µM; 20 min) and to the non-selective β_1- and β_2- adrenoceptor blocker propranolol (100 µM; 20 min) under experimental conditions similar to those described above (Figure 1). Metoprolol reduced $hK_{2P}2.1$ currents by 18.8 ± 2.5% (n = 13; P = 0.0003) and propranolol blocked the channels by 31.2 ± 3.7% (n = 14; P = 0.001) (Figure 2F).

Carvedilol targets $hK_{2P}10.1$ (TREK2) channels

To further elucidate the pharmacological profile of carvedilol, its effects on human $K_{2P}10.1$ channels were analysed in oocytes. Concentration-dependent inhibition of $K_{2P}10.1$ current was revealed using the experimental approach described above (Figure 3A–D) and the derived IC_{50} value

Table 1

Sensitivity to carvedilol of wild-type K_{2P} channels and of subunits generated by alternative mRNA translation initiation

Subunit	$IC_{50,oocytes}$ (mean ± SEM)	Relative drug sensitivity (full-length channel/ truncated subunit)	$IC_{50,HEK}$ (mean ± SEM)
$hK_{2P}2.1$			
$hK_{2P}2.1$ WT	20.3 ± 1.5 μM	–	1.6 ± 0.9 μM
$hK_{2P}2.1$ M57I	16.5 ± 3.7 μM	–	NI
$hK_{2P}2.1$ Δ1–56	79.0 ± 33.8 μM	4.8	NI
$hK_{2P}10.1$			
$hK_{2P}10.1$ WT	24.0 ± 11.1 μM	–	7.6 ± 0.2 μM
$hK_{2P}10.1$ M60I M72I	17.5 ± 4.3 μM	–	NI
$hK_{2P}10.1$ Δ1–59 M72I	45.5 ± 34.2 μM	2.6	NI
$hK_{2P}10.1$ Δ1–71	87.0 ± 66.3 μM	5.0	NI

NI, not investigated; WT, wild type.

(Figure 3C), with n_H of 2.2 ± 1.0, from a series of 6–7 cells is shown in Table 1. Currents were stable during a 20-min control period ($I_{0\,min}$, 1.73 ± 0.23 μA; $I_{20\,min}$, 1.65 ± 0.2 μA = 12; P = 0.12). During carvedilol application (100 μM), $K_{2P}10.1$ currents decreased by 67.5 ± 3.3% (n = 7; P = 0.0007) (Figure 3D). Current inhibition was reduced to 40.5 ± 10.0% during washout, indicating partial reversibility of block. Analysis of $K_{2P}10.1$ current-voltage (I–V) relationships yielded a negligible change of 1.1 mV towards more negative potentials in the presence of carvedilol ($V_{50\%,K2P,control}$ = 25.5 ± 1.2 mV; $V_{50\%,K2P,carvedilol}$ = 24.4 ± 1.0 mV; n = 7; P = 0.02) (Figure 3E,F).

Concentration-dependent blockade of $hK_{2P}2.1$ and $hK_{2P}10.1$ channels in mammalian cells

To evaluate the physiological significance of drug-receptor interactions, concentration-response relationships obtained from mammalian expression systems are required. $K_{2P}2.1$ and $K_{2P}10.1$ potassium channels were expressed in HEK 293 cells to analyse channel sensitivities to carvedilol (Figure 4). From a holding potential of –80 mV, pulses were applied for 500 ms to voltages between –120 and +80 mV in 20 mV increments (0.2 Hz). Following current equilibration (10 min), the degree of inhibition was determined at +60 mV 10 min after carvedilol application (Figure 4A,B,D,E). For HEK 293 cells, the IC_{50} values for blockade of $hK_{2P}2.1$ channels (Hill coefficient n_H = 0.61 ± 0.20; Figure 4C) and for $hK_{2P}10.1$ background channels (Hill coefficient n_H = 1.26 ± 0.06; Figure 4F) are given in Table 1. Four to eight cells were investigated at each concentration. Steady-state outward currents recorded in the presence of 100 μM carvedilol were blocked by 89.4 ± 4.0% ($hK_{2P}2.1$; n = 4; P = 0.17) and by 96.6 ± 1.5% ($hK_{2P}10.1$; n = 4; P = 0.04).

Alternative translation initiation regulates K_{2P} channel sensitivity to carvedilol

Alternative translation initiation generates two ($K_{2P}2.1$) and three ($K_{2P}10.1$) functionally different K_{2P} ion channel subunits respectively (Figure 5A–E) (Simkin *et al.*, 2008; Thomas *et al.*, 2008; Staudacher *et al.*, 2011a). Immunoblot analysis of tissue-specific total protein samples revealed significant $K_{2P}2.1$ protein expression in adult human heart in addition to brain, aorta, skeletal muscle, stomach, small intestine, uterus and prostate (Figure 5C). Furthermore, the presence of a smaller $K_{2P}2.1$ band (which may correspond to truncated $K_{2P}2.1$ channels produced by ATI) was detected in the heart and other tissues (Figure 5C). $K_{2P}10.1$ protein analysis was not performed as reliable cardiac immunoblot protocols and antibodies have not yet been established. To study differential pharmacological effects of carvedilol on K_{2P} isoforms, mutant subunits that specifically produce full-length channels by elimination of downstream start codons were used ($K_{2P}2.1$ M57I; $K_{2P}10.1$ M60I M72I). Drug effects on these channels were compared with truncated subunits associated with ATI ($K_{2P}2.1$ Δ1–56; $K_{2P}10.1$ Δ1–59 M72I; $K_{2P}10.1$ Δ1–71). Figures 5B and E provide an overview of the channels investigated. Using the experimental approach described in Figures 1 and 3, marked differences in drug affinity were detected. Carvedilol (100 μM) reduced full-length $hK_{2P}2.1$ M57I currents by 72.6 ± 3.3% (n = 10; P = 0.0002; Figure 6A,B) compared with 40.7 ± 3.7% inhibition of truncated $hK_{2P}2.1$ Δ1–56 channels (n = 10; P = 0.0001; Figure 6F,G). The corresponding IC_{50} values for blockade of $hK_{2P}2.1$ M57I channels (Hill coefficient n_H = 1.4 ± 0.5; Figure 6C) and of $hK_{2P}2.1$ Δ1–56 channels (Hill coefficient n_H = 1.5 ± 0.6; Figure 6H) are shown in Table 1. Four to 10 cells were investigated at each concentration. Carvedilol inhibition of full-length and truncated $K_{2P}2.1$ variants ($K_{2P}2.1$ M57I and $K_{2P}2.1$ Δ1–56) was statistically compared. The resulting P-values (Table 2) illustrate statistically significant differences in the degree of blockade at concentrations >1 μM, providing statistical support for different drug affinities between full-length and truncated $K_{2P}2.1$ channel variants. Please note that significant differences at 0.1 and 1 μM carvedilol are not expected as there was virtually no inhibition of either subunit at these concentrations (Figure 6C,H). Activation voltages of both $K_{2P}2.1$ isoforms were virtually unchanged in the presence of 100 μM carvedilol (M57I; $V_{50\%,K2P,control}$ = 28.1 ± 0.3 mV; $V_{50\%,K2P,carvedilol}$ = 26.0

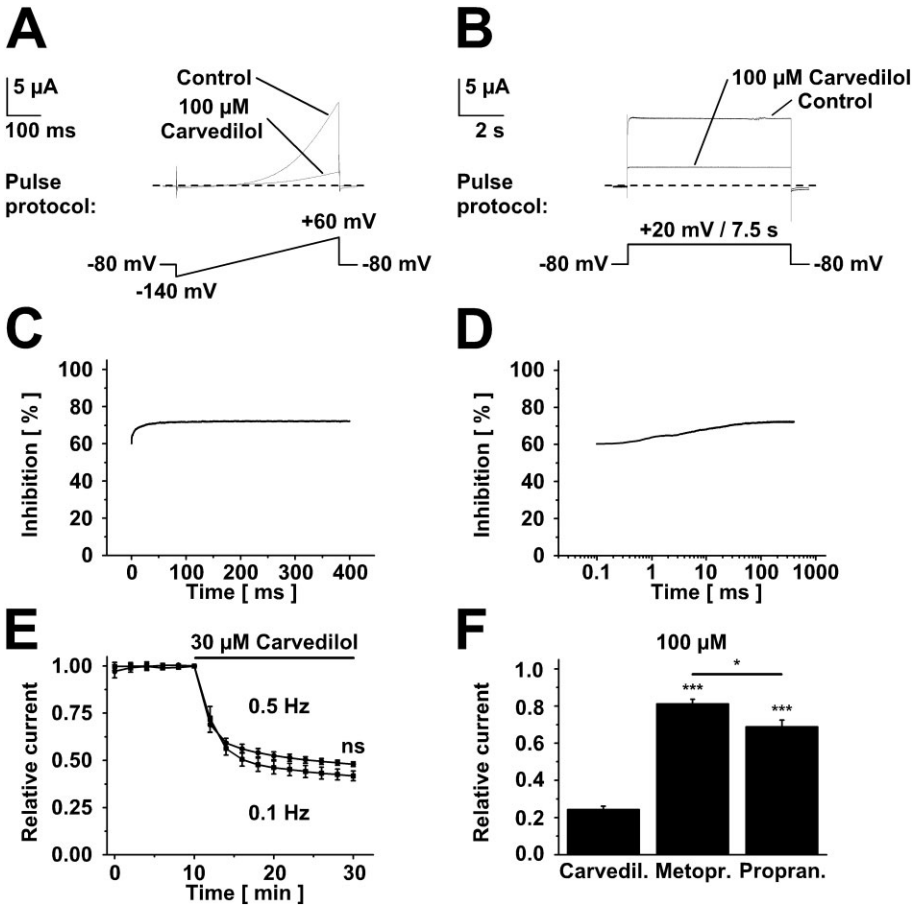

Figure 2

Biophysical characteristics of hK_{2P}2.1 blockade by carvedilol in oocytes. (A) Open rectification of K_{2P}2.1 currents evoked by voltage ramps from –140 to +60 mV. Typical recordings in the absence of the drug and after superfusion with 100 µM carvedilol (20 min) are superimposed. (B–D) Blockade during extended voltage pulses. Currents activated by 7.5 s depolarizing voltage steps to +20 mV are shown under control conditions and after administration of 100 µM carvedilol (20 min). (C, D) The extent of current inhibition during the first 400 ms of the depolarizing voltage step is displayed as % (C, linear time scale; D, logarithmic time scale). (E) Carvedilol block of K_{2P}2.1 is frequency-independent. Relative current amplitudes recorded at +20 mV membrane potential during carvedilol application (0.5 and 0.1 Hz stimulation rates) are plotted versus time (n = 7 oocytes were studied at each rate). For the purpose of clear presentation, not all measurements are displayed. (F) Effects of metoprolol and propranolol on K_{2P}2.1 channels. Mean relative current amplitudes after administration of 100 µM carvedilol (Carvedil; n = 15), 100 µM metoprolol (Metopr; n = 13) and 100 µM propranolol (Propan; n = 14) are displayed. K_{2P} current inhibition by carvedilol was significantly greater than those induced by metoprolol and propranolol (*P < 0.05 vs. metoprolol; ***P < 0.001 vs. carvedilol). Dashed lines indicate zero current levels.

Table 2

Statistical comparisons of relative current inhibition by a range of carvedilol concentrations between full-length (K_{2P}2.1 M57I) and truncated (K_{2P}2.1 Δ1–56) hK_{2P}2.1 channel variants

	0.1 µM	1 µM	10 µM	100 µM	300 µM
P-value (n, hK_{2P}2.1 M57I; n, hK_{2P}2.1 Δ1–56)	0.19^{ns} (10; 8)	0.21^{ns} (10; 6)	0.002** (9; 8)	<0.0001*** (10; 10)	0.014* (10; 4)

*P < 0.05; **P < 0.01; ***P < 0.001; ns, not statistically significant.

± 0.3 mV; n = 10; P < 0.001; Δ1–56; $V_{50\%,K2P,control}$ = 31.2 ± 0.4 mV; $V_{50\%,K2P,carvedilol}$ = 29.7 ± 0.7 mV; n = 10; P = 0.058).

ATI-derived K_{2P}10.1 channel isoforms were differentially regulated by carvedilol as well (Figure 7). Representative current traces are shown for control conditions (Figure 7A,F,K) and after application of 100 µM carvedilol (Figure 7B,G,L) for indicated subunits. Currents were blocked by 69.7 ± 3.5% (K_{2P}10.1 M60I M72I; n = 7; P = 0.001), by 45.3 ± 4.6% (K_{2P}10.1 Δ1–59 M72I; n = 8; P = 0.0002) and by 26.5 ± 1.1% (K_{2P}10.1 Δ1–71; n = 7; P = 0.002) respectively. The IC_{50}

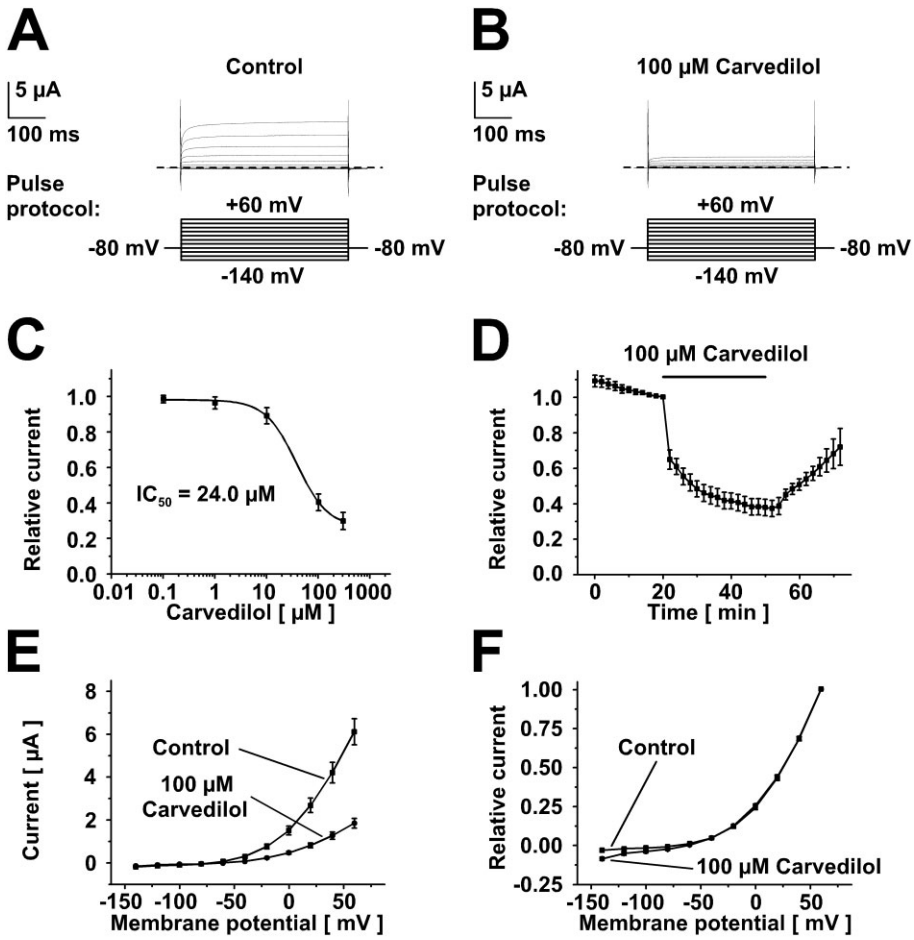

Figure 3

Human $K_{2P}10.1$ (TREK2) channels in oocytes are sensitive to carvedilol. Analyses performed as described in Figure 1 illustrate concentration-dependent $K_{2P}10.1$ current inhibition (A–C; n = 6–7 cells). Zero current levels are indicated by dashed lines. (D) Time course of blockade by 100 µM carvedilol (n = 7). Open rectification (E, F) and current-voltage relationships of $K_{2P}10.1$ channels were not markedly affected by carvedilol (100 µM; n = 7).

Table 3

Statistical comparisons of relative current inhibition by indicated carvedilol concentrations between full-length ($hK_{2P}10.1$ M60I M72I) and truncated ($hK_{2P}10.1$ Δ1–59 M72I, $hK_{2P}10.1$ Δ1–71) $hK_{2P}10.1$ channel variants

	0.1 µM	1 µM	10 µM	100 µM	300 µM
P-value (n, $hK_{2P}10.1$ M60I M72I; n, $hK_{2P}10.1$ Δ1–59 M72I)	0.013* (7;6)	0.032^{ns} (6;7)	0.001** (6;6)	0.001** (7;8)	0.086^{ns} (7;7)
P-value (n, $hK_{2P}10.1$ M60I M72I; n, $hK_{2P}10.1$ Δ1–71)	0.87^{ns} (7;6)	0.20^{ns} (6;7)	0.001** (6;8)	<0.0001*** (7;7)	<0.0001*** (7;7)
P-value (n, $hK_{2P}10.1$ Δ1–59 M72I; n, $hK_{2P}10.1$ Δ1–71)	0.18^{ns} (6;6)	0.26^{ns} (7;7)	0.60^{ns} (6;8)	0.002** (8;7)	0.006* (7;7)

*P < 0.05 (adjusted to 0.05/3 = 0.017); **P < 0.01 (adjusted to 0.01/3 = 0.003); ***P < 0.001 (adjusted to 0.001/3 = 0.0003); ns, not statistically significant; ANOVA with Bonferroni adjustment.

values for block of $hK_{2P}10.1$ M60I M72I (n_H = 1.3 ± 0.4; n = 6–7) and of $hK_{2P}10.1$ Δ1–59 M72I (n_H = 0.97 ± 0.3; n = 6–8) and of $hK_{2P}10.1$ Δ1–71 (n_H = 0.8 ± 0.3; n = 6–8) channels are shown in Table 1. Statistically significant differences between inhibition of full-length channels ($K_{2P}10.1$ M60I M72I) and both truncated variants (K2P10.1 Δ1–59 M72I, $K_{2P}10.1$ Δ1–71) were observed at 100 µM carvedilol (Table 3), confirming different drug sensitivity at concentrations close to the respective IC_{50}

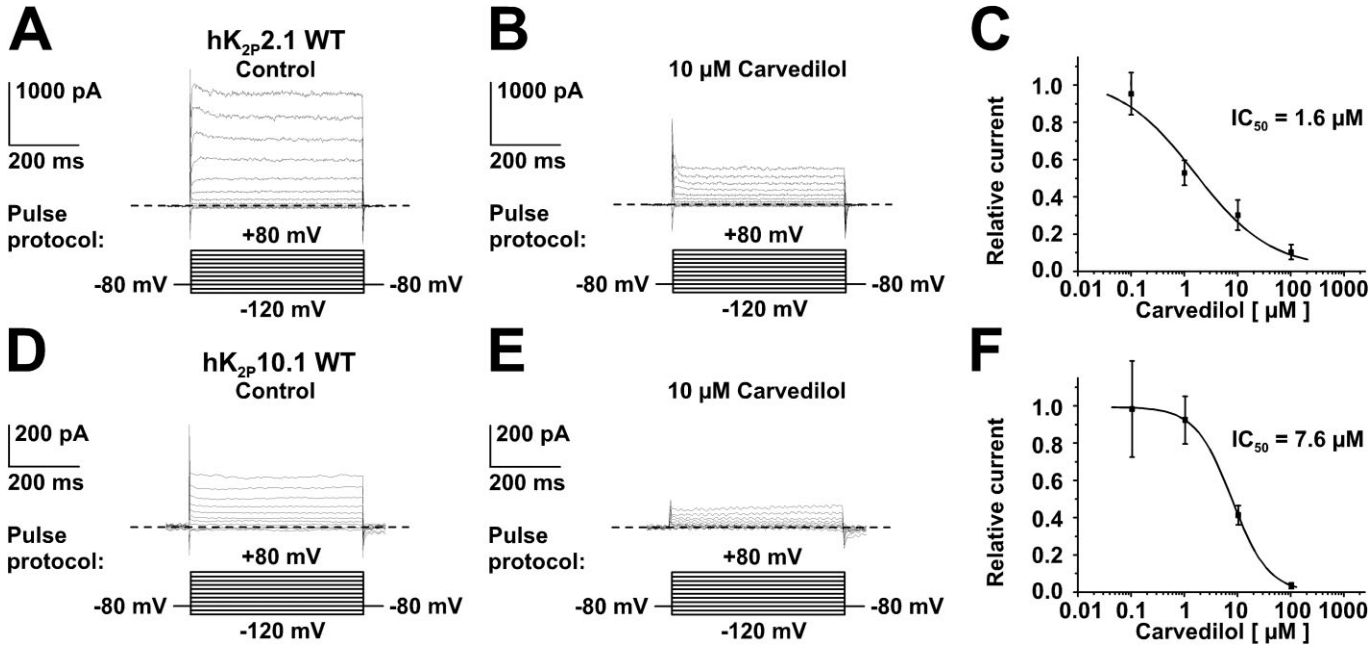

Figure 4

Inhibition of $hK_{2P}2.1$ and $hK_{2P}10.1$ currents expressed in HEK293 cells. Representative $K_{2P}2.1$ and $K_{2P}10.1$ measurements before (A, D) and after exposure to 10 µM carvedilol (B, E) are displayed. (C, F) Concentration-response relationships indicating IC_{50} values of respective K_{2P} channels (n = 4–8 cells).

values. *I–V* relationships of all $K_{2P}10.1$ variants tested were not markedly modified by 100 µM carvedilol ($K_{2P}10.1$ M60I M72I; $V_{50\%,K2P,control}$ = 25.9 ± 0.6 mV; $V_{50\%,K2P,carvedilol}$ = 25.0 ± 0.5 mV; n = 7; P = 0.04; $K_{2P}10.1$ Δ1–59 M72I; $V_{50\%,K2P,control}$ = 30.3 ± 0.4 mV; $V_{50\%,K2P,carvedilol}$ = 27.8 ± 0.4 mV; n = 8; P = 0.001; $K_{2P}10.1$ Δ1–71; $V_{50\%,K2P,control}$ = 30.7 ± 0.4 mV; $V_{50\%,K2P,carvedilol}$ = 29.3 ± 0.5 mV; n = 7; P = 0.005; Figure 7D,I,N).

Discussion

Carvedilol inhibits $hK_{2P}2.1$ (TREK1) and $hK_{2P}10.1$ (TREK2) K_{2P} channels

We report concentration-dependent inhibition of $hK_{2P}2.1$ and $hK_{2P}10.1$ currents by carvedilol with IC_{50} values of 20.3 and 24.0 µM obtained from *Xenopus laevis* oocytes (Table 1). An extension of these findings to I_{TREK1} and I_{TREK2} recorded from mammalian HEK 293 cells revealed IC_{50} values of 1.6 and 7.6 µM respectively. Differences in IC_{50} values between mammalian cells and oocytes are commonly observed and attributed to specific properties of oocytes (e.g. the vitelline membrane and the yolk) that reduce drug affinities. Different $IC_{50,oocytes}/IC_{50,mammalian\ cells}$ ratios are primarily determined by physicochemical drug characteristics. Here, these ratios yield 12.7 ($hK_{2P}2.1$) and 3.2 ($hK_{2P}10.1$) for the same drug, carvedilol, suggesting that channel-specific mechanisms of drug access to the putative receptor site within the pore are affected by oocyte properties as well. During therapeutic application of the drug, total plasma levels between 47 and 615 nM have been measured (McPhillips *et al.*, 1988; Morgan *et al.*, 1990; Gehr *et al.*, 1999; Karle *et al.*, 2001). Carvedilol is approximately 98% bound to plasma proteins, reducing effective free drug concentrations to 0.94–12.3 nM, which would suggest a minimal effect of K_{2P} channel blockade on cardiac electrophysiology under normal pharmacokinetic conditions.

Biophysical properties of $hK_{2P}2.1$ blockade by carvedilol

The biophysical mechanism of $K_{2P}2.1$ inhibition by carvedilol was analysed in detail. A rapid onset of block supports a direct drug-channel interaction as opposed to increased protein turnover or accelerated channel degradation as a molecular mechanism of action. In addition, carvedilol might indirectly affect $K_{2P}2.1$ or $K_{2P}10.1$ function through inhibition of β-adrenoreceptor signalling in oocytes or HEK 293 cells. However, this mechanism appears unlikely as activation of the cAMP/PKA system caused $K_{2P}2.1$ and $K_{2P}10.1$ current reduction, rather than enhancement (Gu *et al.*, 2002; Honoré *et al.*, 2002; Murbartián *et al.*, 2005). Furthermore, functional data suggest that levels of endogenous β-adrenoreceptors are negligible (Kathöfer *et al.*, 2000). The lack of complete $K_{2P}2.1$ and $K_{2P}10.1$ current inhibition in oocytes compared with mammalian cells may be attributed to specific lipophilic properties of the oocyte expression system. Open rectification that is characteristic to K_{2P} channel function in physiological ionic conditions was observed before and during drug block. Finally, the lack of frequency-dependence of $K_{2P}2.1$ channel blockade supports continuous accessibility of the putative drug binding site inside the channel. It is likely that kinetics of drug block (Figure 2) were largely independent of channel opening as the cytosolic channel gate is constitutively open

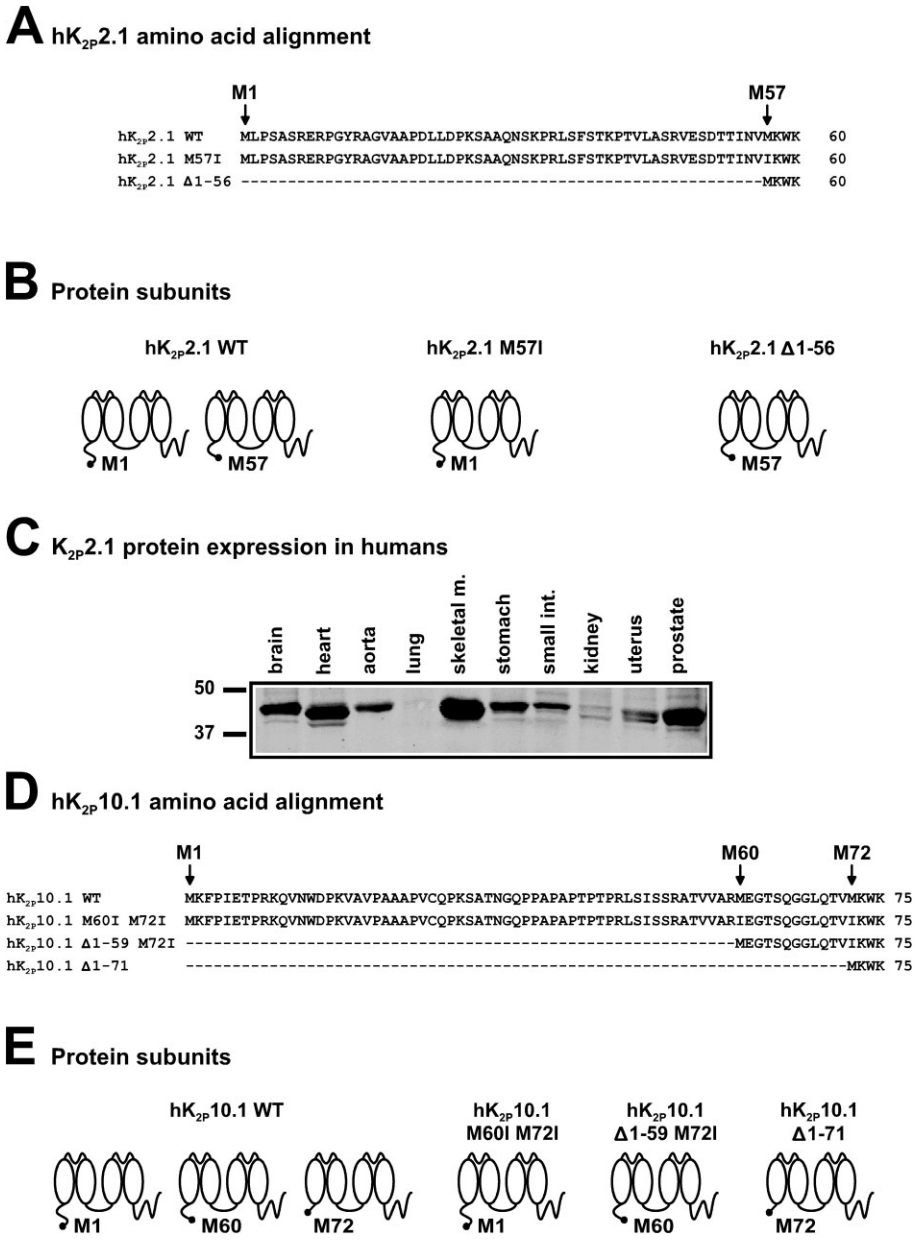

Figure 5

Alternative translation initiation of $hK_{2P}2.1$ and $hK_{2P}10.1$ mRNA produces multiple channel isoforms. (A, D) N terminal amino acid sequence alignments of wild-type (WT) $K_{2P}2.1$ (A) and $K_{2P}10.1$ channels (D). Alternative translation initiation sites are indicated by arrows. In addition, alignments of mutated channels used to specifically produce full-length or truncated K_{2P} proteins in isolation are shown. (B, E) The topologies of $K_{2P}2.1$ (B) and $K_{2P}10.1$ (E) WT channels (left) and of protein variants arising from alternative mRNA translation initiation studied in this work (right) are displayed. (C) Expression of two $K_{2P}2.1$ protein isoforms in indicated human tissues (skeletal m., skeletal muscle; small int., small intestine) visualized by Western blot analysis using an antibody to the $K_{2P}2.1$ C terminus. Markers correspond to apparent molecular weights: 50, 50 kDa; 37, 37 kDa.

(Piechotta *et al.*, 2011; Brohawn *et al.*, 2012; Miller and Long, 2012), allowing for drug binding within the channel pore in state-independent manner.

ATI determines drug sensitivity of K_{2P} channels

This work identifies ATI as a genetic mechanism regulating sensitivity of $K_{2P}2.1$ and $K_{2P}10.1$ channels to carvedilol. Compared with full-length K_{2P} channels, truncated isoforms produced by ATI were 2.6 to 5.0-fold less sensitive to the drug (Table 1). These findings are in line with a previous report describing decreased sensitivity (by 70%) of truncated $K_{2P}2.1$ channels to the antidepressant drug fluoxetine (Eckert *et al.*, 2011). The present study extends regulation of K^+ channel drug sensitivity by ATI to cardiac K_{2P} channels and to a cardiovascular drug, suggesting a broader role of this

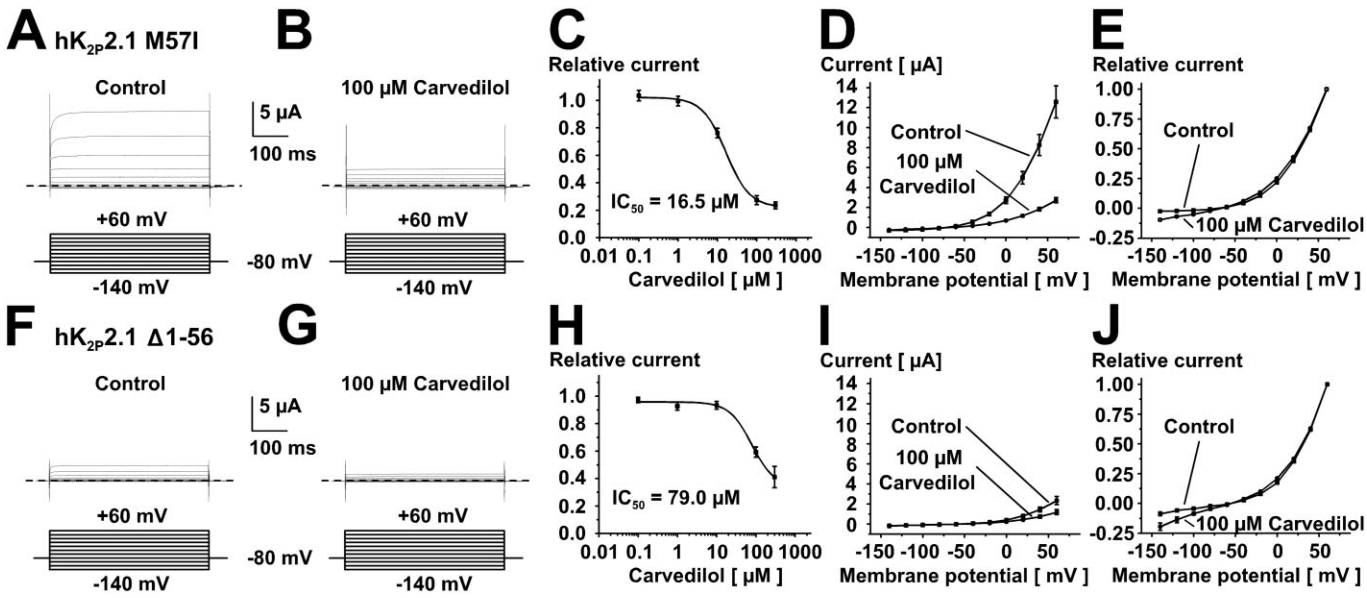

Figure 6

Human K_{2P}2.1 variants produced by ATI exhibit different carvedilol affinity. Channels were studied in *Xenopus* oocytes using indicated voltage protocols. (A, B, F, G) Representative current recordings under control conditions (A, F) and after 20 min perfusion with 100 µM carvedilol (B, G) are illustrated for indicated isoforms. Concentration-response relationships show a 4.8-fold higher IC_{50} value for K_{2P}2.1 Δ1–56 (H) compared with K_{2P}2.1 M57I (C) (n = 6 to 10 cells analysed at each concentration). (D, E, I, J) Voltage-dependence of activation before and after carvedilol application (D, I, original current amplitudes; E, J, values normalized to maximum currents; n = 10). Dashed lines indicate zero current level.

pharmacological mechanism. Several studies have identified the C-terminus of K_{2P}2.1 channels as a critical region for polymodal channel regulation (Honoré, 2007). Reduced carvedilol affinity observed in N-terminally truncated isoforms now indicates a significant contribution of the N-terminus of K_{2P}2.1 and K_{2P}10.1 channels. Truncated K_{2P}2.1 ATI variants may exhibit reduced carvedilol sensitivity, because of the additional Na^+ conductance of the channel pore (Thomas *et al.*, 2008). However, this mechanism could not explain reduced sensitivity among K_{2P}10.1 ATI variants, as loss of K^+ selectivity has not been demonstrated for this channel.

The apparent role of the N-terminus in K_{2P} channel regulation is in line with data obtained from human ether-a-go-go-related gene (hERG) K^+ channels. The length of the hERG channel N-terminus is determined by mRNA splicing (as opposed to ATI-dependent regulation of the K_{2P}2.1 N-terminus reported in the present work). The transcript variant hERG 1b is characterized by a shortened N-terminus and displays reduced affinity to the class III compounds dofetilide and E-4031 (Abi-Gerges *et al.*, 2011). It is reasonable to assume that reduced length of the N-terminus modulates drug sensitivity through alterations of the channel pore structure that contains the putative binding site. As the N-terminus is not detailed in the crystal structures of K_{2P}1.1 and mechanosensitive K_{2P}4.1 channels, the precise mechanism by which the N-terminus regulates K_{2P} channel pharmacology remains to be elucidated (Brohawn *et al.*, 2012; Miller and Long, 2012).

Clinical implications

Class III antiarrhythmic drugs suppress atrial fibrillation and ventricular tachyarrhythmia through K^+ channel block, resulting in prevention of electrical reentry via prolongation of action potential duration and cardiac refractoriness. Outward potassium currents mediated by K_{2P} channels contribute to cardiac repolarization. Thus, inhibition of cardiac K_{2P} channels represents a novel concept in antiarrhythmic therapy, with carvedilol blockade of hK_{2P}2.1 and hK_{2P}10.1 K^+ currents observed in the current study and inhibition of hK_{2P}3.1 channels reported previously (Staudacher *et al.*, 2011b) serving as proof of this principle. The specific contribution of K_{2P} channel blockade to the antiarrhythmic efficacy of carvedilol in heart failure and atrial fibrillation patients (Senior *et al.*, 1992; Brunvand *et al.*, 1996; Cice *et al.*, 2000; Takusagawa *et al.*, 2000; Katritsis *et al.*, 2003; Merritt *et al.*, 2003; Ramaswamy, 2003; Haghjoo *et al.*, 2007; Acikel *et al.*, 2008), however, is expected to be low, as the IC_{50} values determined *in vitro* in the low micromolar range were much higher than the nanomolar free therapeutic drug concentrations found in clinical practice. Compared with K_{2P}2.1 (IC_{50} = 1.6 µM) and K_{2P}10.1 channels (IC_{50} = 7.6 µM), higher sensitivity implying greater clinical effect was demonstrated for the K_{2P}3.1 channels (IC_{50} = 0.8 µM; Staudacher *et al.*, 2011b). The overall antiarrhythmic efficacy of the drug is likely to result primarily from its anti-adrenergic properties, supported by multichannel blocking effects on potassium currents (I_{Kr}, I_{Ks}, I_{to}, I_{Kur}, I_{TASK1}, I_{TREK1}, I_{TREK2}, $I_{K,ATP}$), pacemaker current (I_f), L-type calcium current and the cardiac ryanodine receptor with different affinities (Cheng *et al.*, 1999; Kawakami *et al.*, 2006; Kikuta *et al.*, 2006; Deng *et al.*, 2007; Yokoyama *et al.*, 2007; Staudacher *et al.*, 2011b; Zhou *et al.*, 2011).

In conclusion, this investigation showed inhibition of K_{2P}2.1 and K_{2P}10.1 channels by carvedilol, providing proof-of-concept to support a pharmacological role of cardiac K_{2P}

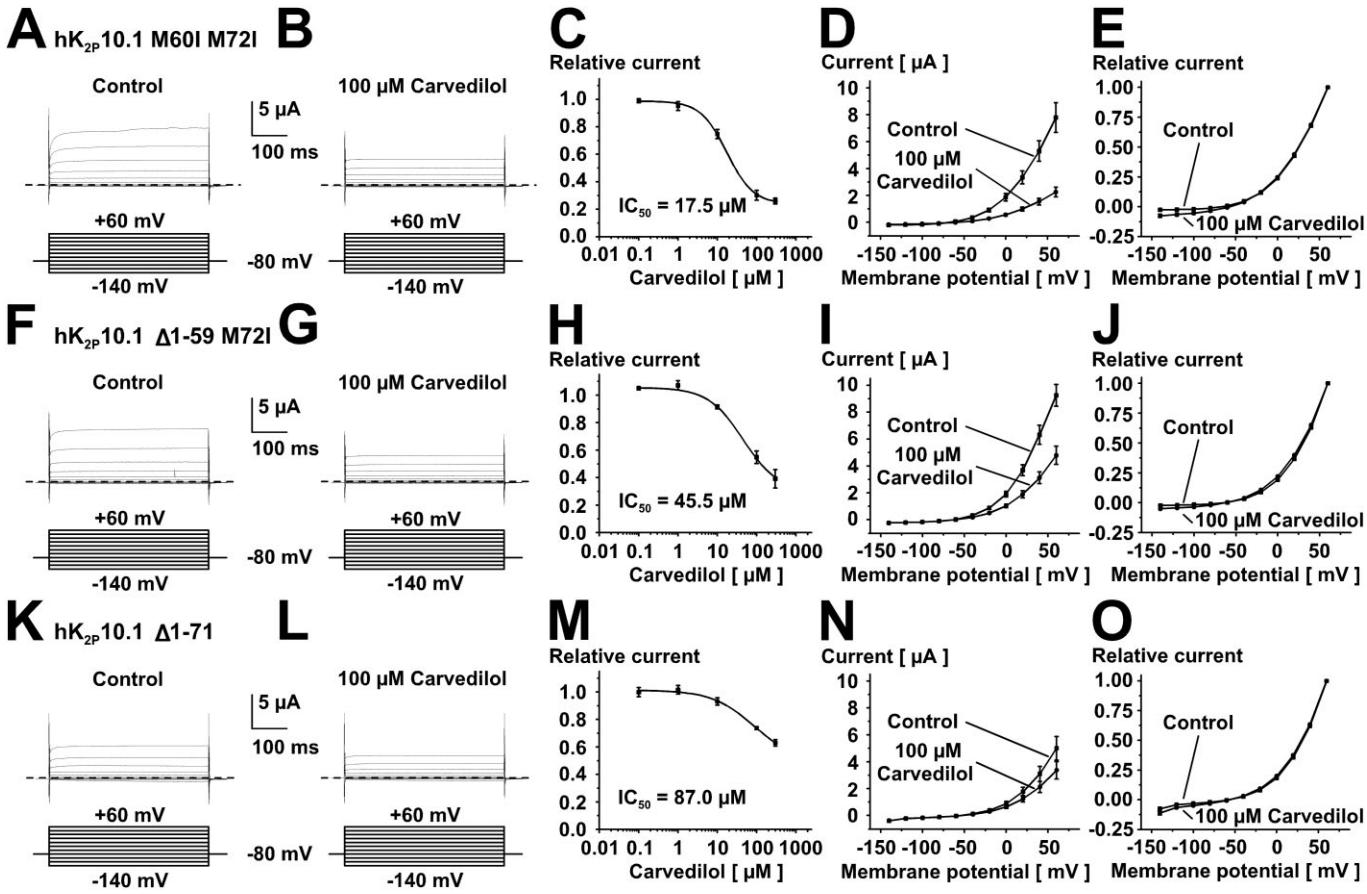

Figure 7

ATI affects inhibition of $hK_{2P}10.1$ channels by carvedilol. Representative macroscopic recordings from oocytes and activation curves reflect blockade of full-length ($K_{2P}10.1$ M60I M72I; A, B, D, E) and of two truncated isoforms ($K_{2P}10.1$ Δ1–59 M72I; F, G, I, J; $K_{2P}10.1$ Δ1–71; K, L, N, O) by 100 µM carvedilol. Zero current levels are marked by dashed lines. Corresponding concentration-response curves demonstrate decreased carvedilol sensitivity of truncated isoforms (H, M) compared with full-length channels (C) (n = 7 to 8 cells were studied).

channels as antiarrhythmic drug targets. The therapeutic significance of K_{2P} channel blockade in heart rhythm disorders requires validation in translational and clinical studies. At the molecular level, antiarrhythmic drug sensitivity is determined by alternative translation initiation of $K_{2P}2.1$ and $K_{2P}10.1$ mRNA that produces subunits with different carvedilol affinity. Differential expression of ATI-dependent K_{2P} channel variants may result in spatiotemporal variation of electrophysiological carvedilol effects in the heart. In addition, the effect of ATI on antiarrhythmic drug efficacy has broad and general implications for cardiac drug discovery.

Acknowledgements

We gratefully acknowledge the generous support of Dr. Steve Goldstein with $K_{2P}2.1$ immunoblots, and we thank Jennifer Gütermann, Christine Jeckel and Bianca-Sarah Stadler for excellent technical help. This study was supported in part by research grants from the German Heart Foundation/German Foundation of Heart Research (to D. T.), from the Joachim Siebeneicher Foundation (to D. T.) and from the DZHK (Deutsches Zentrum für Herz-Kreislauf-Forschung – German Centre for Cardiovascular Research) and the BMBF (German Ministry of Education and Research) (to H. A. K. and D. T.).

Conflict of interest

None declared.

References

Abi-Gerges N, Holkham H, Jones EM, Pollard CE, Valentin JP, Robertson GA (2011). hERG subunit composition determines differential drug sensitivity. Br J Pharmacol 164: 419–432.

Acikel S, Bozbas H, Gultekin B, Aydinalp A, Saritas B, Bal U *et al.* (2008). Comparison of the efficacy of metoprolol and carvedilol for preventing atrial fibrillation after coronary bypass surgery. Int J Cardiol 126: 108–113.

Aimond F, Rauzier JM, Bony C, Vassort G (2000). Simultaneous activation of p38 MAPK and p42/44 MAPK by ATP stimulates the K^+ current I_{TREK} in cardiomyocytes. J Biol Chem 275: 39110–39116.

Alexander SPH, Benson HE, Faccenda E, Pawson AJ, Sharman JL, Catterall WA *et al*. (2013). The Concise Guide to PHARMACOLOGY 2013/14: Ion Channels. Br J Pharmacol 170: 1607–1651.

Bockenhauer D, Zilberberg N, Goldstein SA (2001). KCNK2: reversible conversion of a hippocampal potassium leak into a voltage-dependent channel. Nat Neurosci 4: 486–491.

Brohawn SG, del Mármol J, MacKinnon R (2012). Crystal structure of the human K_{2P} TRAAK, a lipid- and mechano-sensitive K^+ ion channel. Science 335: 436–441.

Brunvand H, Frłyland L, Hexeberg E, Rynning SE, Berge RK, Grong K (1996). Carvedilol improves function and reduces infarct size in the feline myocardium by protecting against lethal reperfusion injury. Eur J Pharmacol 314: 99–107.

Cheng J, Niwa R, Kamiya K, Toyama J, Kodama I (1999). Carvedilol blocks the repolarizing K + currents and the L-type Ca2+ current in rabbit ventricular myocytes. Eur J Pharmacol 376: 189–201.

Cice G, Tagliamonte E, Ferrara L, Iacono A (2000). Efficacy of carvedilol on complex ventricular arrhythmias in dilated cardiomyopathy: double-blind, randomized, placebo-controlled study. Eur Heart J 21: 1259–1264.

Decher N, Wemhöner K, Rinné S, Netter MF, Zuzarte M, Aller MI *et al*. (2011). Knock-out of the potassium channel TASK-1 leads to a prolonged QT interval and a disturbed QRS complex. Cell Physiol Biochem 28: 77–86.

Deng C, Yu X, Kuang S, Zhang W, Zhou Z, Zhang K *et al*. (2007). Effects of carvedilol on transient outward and ultra-rapid delayed rectifier potassium currents in human atrial myocytes. Life Sci 80: 665–671.

Donner BC, Schullenberg M, Geduldig N, Hüning A, Mersmann J, Zacharowski K *et al*. (2011). Functional role of TASK-1 in the heart: studies in TASK-1-deficient mice show prolonged cardiac repolarization and reduced heart rate variability. Basic Res Cardiol 106: 75–87.

Eckert M, Egenberger B, Döring F, Wischmeyer E (2011). TREK-1 isoforms generated by alternative translation initiation display different susceptibility to the antidepressant fluoxetine. Neuropharmacology 61: 918–923.

Fink M, Duprat F, Lesage F, Reyes R, Romey G, Heurteaux C *et al*. (1996). Cloning, functional expression and brain localization of a novel unconventional outward rectifier K + channel. EMBO J 15: 6854–6862.

Gehr TW, Tenero DM, Boyle DA, Qian Y, Sica DA, Shusterman NH (1999). The pharmacokinetics of carvedilol and its metabolites after single and multiple dose oral administration in patients with hypertension and renal insufficiency. Eur J Clin Pharmacol 55: 269–277.

Gierten J, Ficker E, Bloehs R, Schlömer K, Kathöfer S, Scholz E *et al*. (2008). Regulation of two-pore-domain (K_{2P}) potassium leak channels by the tyrosine kinase inhibitor genistein. Br J Pharmacol 154: 1680–1690.

Gierten J, Ficker E, Bloehs R, Schweizer PA, Zitron E, Scholz E *et al*. (2010). The human cardiac K_{2P}3.1 (TASK-1) potassium leak channel is a molecular target for the class III antiarrhythmic drug amiodarone. Naunyn Schmiedebergs Arch Pharmacol 381: 261–270.

Gierten J, Hassel D, Schweizer PA, Becker R, Katus HA, Thomas D (2012). Identification and functional characterization of zebrafish K_{2P}10.1 (TREK2) two-pore-domain K + channels. BBA Biomembranes 1818: 33–41.

Goldstein SA, Bockenhauer D, O'Kelly I, Zilberberg N (2001). Potassium leak channels and the KCNK family of two-P-domain subunits. Nat Rev Neurosci 2: 175–184.

Goonetilleke L, Quayle J (2012). TREK-1 K^+ channels in the cardiovascular system: their significance and potential as a therapeutic target. Cardiovasc Ther 30: e23–e29.

Gu W, Schlichthörl G, Hirsch JR, Engels H, Karschin C, Karschin A *et al*. (2002). Expression pattern and functional characteristics of two novel splice variants of the two-pore-domain potassium channel TREK-2. J Physiol 539: 657–668.

Haghjoo M, Saravi M, Hashemi MJ, Hosseini S, Givtaj N, Ghafarinejad MH *et al*. (2007). Optimal beta-blocker for prevention of atrial fibrillation after on-pump coronary artery bypass graft surgery: carvedilol versus metoprolol. Heart Rhythm 4: 1170–1174.

Honoré E (2007). The neuronal background K2P channels: focus on TREK1. Nat Rev Neurosci 8: 251–261.

Honoré E, Maingret F, Lazdunski M, Patel AJ (2002). An intracellular proton sensor commands lipid- and mechano-gating of the K(+) channel TREK-1. EMBO J 21: 2968–2976.

Kanoupakis EM, Manios EG, Mavrakis HE, Kallergis EM, Lyrarakis GM, Koutalas EP *et al*. (2008). Electrophysiological effects of carvedilol administration in patients with dilated cardiomyopathy. Cardiovasc Drugs Ther 22: 169–176.

Karle CA, Kreye VA, Thomas D, Röckl K, Kathöfer S, Zhang W *et al*. (2001). Antiarrhythmic drug carvedilol inhibits HERG potassium channels. Cardiovasc Res 49: 361–370.

Kathöfer S, Zhang W, Karle C, Thomas D, Schoels W, Kiehn J (2000). Functional coupling of human beta 3-adrenoreceptors to the KvLQT1/MinK potassium channel. J Biol Chem 275: 26743–26747.

Katritsis DG, Panagiotakos DB, Karvouni E, Giazitzoglou E, Korovesis S, Paxinos G *et al*. (2003). Comparison of effectiveness of carvedilol versus bisoprolol for maintenance of sinus rhythm after cardioversion of persistent atrial fibrillation. Am J Cardiol 92: 1116–1119.

Kawakami K, Nagatomo T, Abe H, Kikuchi K, Takemasa H, Anson BD *et al*. (2006). Comparison of HERG channel blocking effects of various beta-blockers – implication for clinical strategy. Br J Pharmacol 147: 642–652.

Kilkenny C, Browne W, Cuthill IC, Emerson M, Altman DG (2010). Animal research: Reporting *in vivo* experiments: the ARRIVE guidelines. Br J Pharmacol 160: 1577–1579.

Kikuta J, Ishii M, Kishimoto K, Kurachi Y (2006). Carvedilol blocks cardiac KATP and KG but not IK1 channels by acting at the bundle-crossing regions. Eur J Pharmacol 529: 47–54.

Kisselbach J, Schweizer PA, Gerstberger R, Becker R, Katus HA, Thomas D (2012). Enhancement of K_{2P}2.1 (TREK1) background currents expressed in Xenopus oocytes by voltage-gated K + channel β subunits. Life Sci 91: 377–383.

Li XT, Dyachenko V, Zuzarte M, Putzke C, Preisig-Müller R, Isenberg G *et al*. (2006). The stretch-activated potassium channel TREK-1 in rat cardiac ventricular muscle. Cardiovasc Res 69: 86–97.

Limberg SH, Netter MF, Rolfes C, Rinné S, Schlichthörl G, Zuzarte M *et al*. (2011). TASK-1 channels may modulate action potential duration of human atrial cardiomyocytes. Cell Physiol Biochem 28: 613–624.

Liu W, Saint DA (2004). Heterogeneous expression of tandem-pore K + channel genes in adult and embryonic rat heart quantified by real-time polymerase chain reaction. Clin Exp Pharmacol Physiol 31: 174–178.

McGrath J, Drummond G, McLachlan E, Kilkenny C, Wainwright C (2010). Guidelines for reporting experiments involving animals: the ARRIVE guidelines. Br J Pharmacol 160: 1573–1576.

McPhillips JJ, Schwemer GT, Scott DI, Zinny M, Patterson D (1988). Effects of carvedilol on blood pressure in patients with mild to moderate hypertension. A dose response study. Drugs 36 (Suppl. 6): 82–91.

Medhurst AD, Rennie G, Chapman CG, Meadows H, Duckworth MD, Kelsell RE *et al.* (2001). Distribution analysis of human two pore domain potassium channels in tissues of the central nervous system and periphery. Brain Res Mol Brain Res 86: 101–114.

Merritt JC, Niebauer M, Tarakji K, Hammer D, Mills RM (2003). Comparison of effectiveness of carvedilol versus metoprolol or atenolol for atrial fibrillation appearing after coronary artery bypass grafting or cardiac valve operation. Am J Cardiol 92: 735–736.

Miller AN, Long SB (2012). Crystal structure of the human two-pore domain potassium channel $K_{2P}1$. Science 335: 432–436.

Morgan T, Anderson A, Cripps J, Adam W (1990). Pharmacokinetics of carvedilol in older and younger patients. J Hum Hypertens 4: 709–715.

Murbartián J, Lei Q, Sando JJ, Bayliss DA (2005). Sequential phosphorylation mediates receptor- and kinase-induced inhibition of TREK-1 background potassium channels. J Biol Chem 280: 30175–30184.

Petric S, Clasen L, van Wessel C, Geduldig N, Ding Z, Schullenberg M *et al.* (2012). In vivo electrophysiological characterization of TASK-1 deficient mice. Cell Physiol Biochem 30: 523–537.

Piechotta PL, Rapedius M, Stansfeld PJ, Bollepalli MK, Ehrlich G, Andres-Enguix I *et al.* (2011). The pore structure and gating mechanism of K2P channels. EMBO J 30: 3607–3619.

Poole-Wilson PA, Swedberg K, Cleland JG, Di Lenarda A, Hanrath P, Komajda M *et al.* (2003). Comparison of carvedilol and metoprolol on clinical outcomes in patients with chronic heart failure in the Carvedilol Or Metoprolol European Trial (COMET): randomised controlled trial. Lancet 362: 7–13.

Putzke C, Wemhöner K, Sachse FB, Rinné S, Schlichthörl G, Li XT *et al.* (2007). The acid-sensitive potassium channel TASK-1 in rat cardiac muscle. Cardiovasc Res 75: 59–68.

Rahm AK, Gierten J, Kisselbach J, Staudacher I, Staudacher K, Schweizer PA *et al.* (2012). Protein kinase C-dependent activation of human $K_{2P}18.1$ K^+ channels. Br J Pharmacol 166: 764–773.

Rahm AK, Wiedmann F, Gierten J, Schmidt C, Schweizer PA, Becker R *et al.* (2014). Functional characterization of zebrafish $K_{2P}18.1$ (TRESK) two-pore-domain K^+ channels. Naunyn Schmiedebergs Arch Pharmacol 387: 291–300.

Ramaswamy K (2003). Beta blockers improve outcome in patients with heart failure and atrial fibrillation: U.S. carvedilol study. Card Electrophysiol Rev 7: 229–232.

Ravens U (2010). Novel pharmacological approaches for antiarrhythmic therapy. Naunyn Schmiedebergs Arch Pharmacol 381: 187–193.

Remme WJ, Torp-Pedersen C, Cleland JG, Poole-Wilson PA, Metra M, Komajda M *et al.* (2007). Carvedilol protects better against vascular events than metoprolol in heart failure: results from COMET. J Am Coll Cardiol 49: 963–971.

Reyes R, Duprat F, Lesage F, Fink M, Salinas M, Farman N *et al.* (1998). Cloning and expression of a novel pH-sensitive two pore domain K + channel from human kidney. J Biol Chem 273: 30863–30869.

Sandoz G, Bell SC, Isacoff EY (2011). Optical probing of a dynamic membrane interaction that regulates the TREK1 channel. Proc Natl Acad Sci U S A 108: 2605–2610.

Schmidt C, Wiedmann F, Schweizer PA, Becker R, Katus HA, Thomas D (2012). Novel electrophysiological properties of dronedarone: inhibition of human cardiac two-pore-domain potassium (K_{2P}) channels. Naunyn Schmiedebergs Arch Pharmacol 385: 1003–1016.

Schmidt C, Wiedmann F, Tristram F, Anand P, Wenzel W, Lugenbiel P *et al.* (2014). Cardiac expression and atrial fibrillation-associated remodeling of $K_{2P}2.1$ (TREK-1) K^+ channels in a porcine model. Life Sci 97: 107–115.

Senior R, Müller-Beckmann B, DasGupta P, van der Does R, Lahiri A (1992). Effects of carvedilol on ventricular arrhythmias. J Cardiovasc Pharmacol 19: 117–121.

Seyler C, Duthil-Straub E, Zitron E, Gierten J, Scholz EP, Fink RH *et al.* (2012). TASK1 ($K_{2P}3.1$) K^+ current inhibition by endothelin-1 is mediated by Rho kinase-dependent channel phosphorylation. Br J Pharmacol 165: 1467–1475.

Simkin D, Cavanaugh EJ, Kim D (2008). Control of the single channel conductance of $K_{2P}10.1$ (TREK-2) by the amino-terminus: role of alternative translation initiation. J Physiol 586: 5651–5663.

Staudacher K, Baldea I, Kisselbach J, Staudacher I, Rahm AK, Schweizer PA *et al.* (2011a). Alternative splicing determines mRNA translation initiation and function of human $K_{2P}10.1$ K^+ channels. J Physiol 589: 3709–3720.

Staudacher K, Staudacher I, Ficker E, Seyler C, Gierten J, Kisselbach J *et al.* (2011b). Carvedilol targets human $K_{2P}3.1$ (TASK1) K + leak channels. Br J Pharmacol 163: 1099–1110.

Takusagawa M, Komori S, Matsumura K, Osada M, Kohno I, Umetani K *et al.* (2000). The inhibitory effects of carvedilol against arrhythmias induced by coronary reperfusion in anesthetized rats. J Cardiovasc Pharmacol Ther 5: 105–112.

Tan JH, Liu W, Saint DA (2004). Differential expression of the mechanosensitive potassium channel TREK-1 in epicardial and endocardial myocytes in rat ventricle. Exp Physiol 89: 237–242.

Terrenoire C, Lauritzen I, Lesage F, Romey G, Lazdunski M (2001). A TREK-1-like potassium channel in atrial cells inhibited by beta-adrenergic stimulation and activated by volatile anesthetics. Circ Res 89: 336–342.

Thomas D, Plant LD, Wilkens CM, McCrossan ZA, Goldstein SA (2008). Alternative translation initiation in rat brain yields $K_{2P}2.1$ potassium channels permeable to sodium. Neuron 58: 859–870.

Veale EL, Rees KA, Mathie A, Trapp S (2010). Dominant negative effects of a non-conducting TREK1 splice variant expressed in brain. J Biol Chem 285: 29295–29304.

Yokoyama A, Sato N, Kawamura Y, Hasebe N, Kikuchi K (2007). Electrophysiological effects of carvedilol on rabbit heart pacemaker cells. Int Heart J 48: 347–358.

Zhang H, Shepherd N, Creazzo TL (2008). Temperature-sensitive TREK currents contribute to setting the resting membrane potential in embryonic atrial myocytes. J Physiol 586: 3645–3656.

Zhao LN, Fu L, Gao QP, Xie RS, Cao JX (2011). Regional differential expression of TREK-1 at left ventricle in myocardial infarction. Can J Cardiol 27: 826–833.

Zhou Q, Xiao J, Jiang D, Wang R, Vembaiyan K, Wang A *et al.* (2011). Carvedilol and its new analogs suppress arrhythmogenic store overload-induced Ca^{2+} release. Nat Med 17: 1003–1009.